Characteristics of 3D Micro-Structured Semiconductor High Efficiency Neutron Detectors

S. L. Bellinger, *Member, IEEE*, W. J. McNeil, T. C. Unruh, and D. S. McGregor, *Member, IEEE*

***Abstract*—Silicon diodes with large aspect ratio perforated micro-structures backfilled with ^{6}LiF show a dramatic increase in neutron detection efficiency beyond that of conventional thin-film coated planar devices. Described in the following are advancements in the technology with increased perforation depths. Perforated silicon diodes with three different etched micro-structure patterns were tested for neutron counting efficiency. The etched micro-structure patterns consisted of circular holes, straight trenches, and continuous sinusoidal waves, with each pattern etched 200 μm deep. Normal incident neutron counting efficiencies were determined to be 9.7%, 12.6%, and 16.2% for circular hole, straight trench, and sinusoidal devices, respectively, at a reverse bias of 3 volts. The perforated neutron detectors demonstrate limited sensitivity to high-energy photon irradiation with a ^{60}Co gamma-ray source. This work is part of on-going research to develop solid-state semiconductor neutron detectors with high detection efficiencies and uniform angular responses.**

***Index Terms*—Neutron detectors, perforated diode.**

I. Introduction

PERFORATED micro-structure silicon diode devices, backfilled with neutron reactive materials, have been investigated as high efficiency thermal neutron detectors [1]–[13]. The basic configuration consists of a common *pin* junction diode, which is perforated with patterned micro-structures, and then backfilled with neutron reactive materials. Such devices are compact, easily produced in mass-quantity, have low power requirements, and are far superior to familiar thin-film planar neutron detectors, which are restricted to low thermal neutron detection efficiencies, typically no greater than 4.5% intrinsic efficiency [1], [11]–[16]. In the present work, the neutron reactive material is based on the ^{6}Li(n,t)^{4}He reaction. When thermal neutrons are absorbed in ^{6}Li, a 2.73 MeV triton and a 2.05 MeV helium nucleus are ejected in opposite directions. In comparison to other neutron reactive materials, the reaction products from the ^{6}Li(n,t)^{4}He reaction are far more energetic than those of the $^{10}\mathrm{B}(\mathrm{n},\alpha)^{7}\mathrm{Li}$ or $^{157}\mathrm{Gd}(\mathrm{n},\gamma)^{158}\mathrm{Gd}$ reactions and, hence, are much easier to detect and discriminate from measurable background radiations [7]. Consequently, of the three aforementioned neutron reactive materials commonly used for thin-film coated thermal neutron detectors, the following work concentrates only on devices constructed with ^{6}LiF as the neutron converter material.

With the recent advancements in inductively-coupled-plasma reactive-ion-etching (ICP-RIE) using high-aspect ratio deep etching (HARDE) techniques, unique perforated Si diode micro-structures have been realized [2]–[5]. Current perforated silicon micro-structures, that we have successively etched, include circular hole, straight trench, chevron trench, and sinusoidal trench patterns. The changes in the perforated patterns are due to an evolution in the neutron detector design in response to neutron streaming effects. To improve the uniformity of the angular response of the device, trench designs were developed, eventually leading to the uniform angular response sinusoidal trench design [4], [6]. The afore-mentioned micro-structure patterns, with HARDE techniques, have been successfully etched 200 μm deep in hopes of increasing the neutron detection efficiencies beyond their predecessors, by increasing neutron reactive material volume [1]–[5].

Neutron detection efficiencies for the circular hole, straight trench, and sinusoidal trench micro-structured devices, were experimentally measured with a diffracted thermal neutron beam at the Kansas State University TRIGA Mark II nuclear reactor. Also, to evaluate a high energy gamma-ray response of the perforated neutron detectors, a ^{60}Co irradiation response was experimentally measured for each of the three perforated micro-structure neutron detector designs.

II. Perforated Detector Design

The perforated detectors were manufactured as Si *pip* diodes. The diode fabrication processes were completed on 7.6 cm diameter float zone, single-side polished, $>$ 10 kΩ-cm, n-type Si wafers approximately 325 μm thick. Using a boron nitride solid-source selective diffusion process, shallow p-type junctions, in ν-type grade material, were produced. Previous devices have shown that most of the full energy from the secondary charged particles can be collected with little or no externally applied bias [4]. Perforating the etched structures into the selectively diffused Si diodes, shown in Fig. 1, was accomplished by an ICP-RIE etch process; afterwards, the perforations were passivated by a thermally grown oxide [2]. The perforations were then backfilled with ^{6}LiF material [2].

Two mechanisms increase the efficiency of perforated diodes far beyond common thin-film coated devices. First, intuitively, the probability of neutron absorption increases due to the increased amount of absorbing material in the perforations or "absorber columns" [1], [11]. Second, the probability that secondary charged particles will enter the active volume of the

Manuscript received June 30, 2008; revised August 25, 2008. Current version published June 10, 2009.

The authors are with the SMART Lab., Kansas State University, Manhattan, KS 66506 USA (e-mail: slb3888@ksu.edu).

This work was supported in part by the DTRA under Contract DTRA-01-03-C-0051, in part by the NSF IMR-MIP under Grant 0412208, and in part by the U.S. Department of Energy NEER under Grant DE-FG07-04ID14599.

Digital Object Identifier 10.1109/TNS.2008.2006682

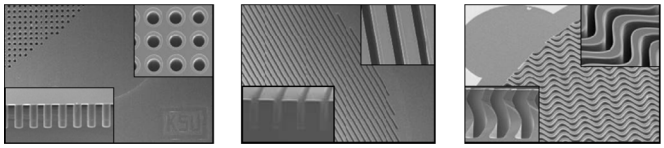

Fig. 1. Shown are three different perforated micro-structure detector designs, from left to right, circular hole, straight trench, and sinusoidal trench.

detector increases substantially due to the small radius of the absorbing columns. Hence, unlike a simple thin-film coated diode, where only one reaction product can enter the detector per interaction, both reaction products can enter the detector, therefore dramatically increasing the output signal from the detector [1], [2], [11].

III. Experimental Procedure

The three perforated detector designs were tested for neutron response at the KSU TRIGA Mark II Nuclear Reactor diffracted thermal neutron beam port. The diffracted thermal neutron beam yielded a flux of 1.2×10^4 neutrons/cm^{2}s as characterized by a ^{3}He (Reuter-Stokes, 5.1 cm dia. by 12.7 cm, 4 atm) cylindrical detector. The ^{3}He detector was assumed to have a thermal neutron detection efficiency of near 100%, such that the axis of the ^{3}He detector was aligned along the neutron beam axis. Though the dead time of the ^{3}He detector was large at the given beam flux, the Maestro-32 software adequately adjusted the live time of the detector; hence, the detector was not limited by high flux dead time.

The neutron beam flux was calibrated before and measured after each neutron detector response experiment, at a steady-state reactor operation, to guarantee consistency in the neutron beam flux. To ensure no hot-spots in the 1.25 cm diameter neutron beam, the uniformity of the neutron beam at the test location was verified by using a neutron sensitive film cassette and observing the resulting unvarying exposure.

A cadmium shutter was used to distinguish the thermal neutron response from fast and epithermal response. A detector reverse bias of 3 volts was applied to all three devices. Basic NIM counting electronics and an MCA were used for data collection. The active detection area for the perforated neutron detectors was 0.28 cm^2 [4].

A. Neutron Counting Efficiency

The neutron detection response for each design was determined by means of dividing the measured response by the count time and the active detection area, as seen within the neutron beam. For the purpose of these efficiency tests, the detector face was orientated perpendicular to the neutron beam. The lower level discriminator (LLD) was chosen for the efficiency calculation such that the measured prompt gamma-ray response from neutron activation in the cadmium shutter was ignored. The calculated neutron response was then divided by the ^{3}He calibration flux to yield the thermal neutron detection efficiency. Neutron counting efficiency error propagation was calculated from the perforated detector summed count variance and the ^{3}He detector summed count variance.

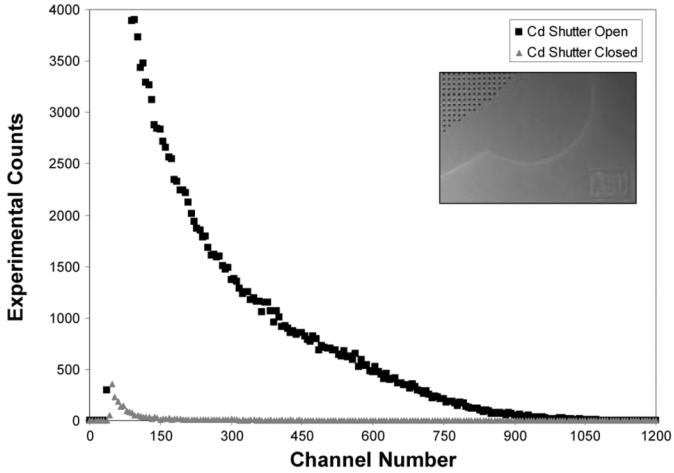

Fig. 2. Data for measured efficiency and spectral features for a circular hole perforated detector with 30 μm diameter 200 μm deep holes filled with ^{6}LiF.

B. Perforated Neutron Detector ^{60}Co Irradiation Response

High energy gamma-ray detection response for each design was found by irradiating each device with a ^{60}Co source, assay 9.031 μCi, Oct. 2003, at a distance of 0.5 cm from the detector face, for 10 minutes. A detector reverse bias of 3 volts was applied to all three devices. The same NIM counting electronics and MCA that were used for the neutron response tests were also used for the high energy gamma-ray response tests. The ^{60}Co gamma-ray response spectrum was then overlaid on a neutron response spectrum collected for 1 hour for response comparisons. An additional high energy gamma-ray irradiation response was found for a 26 μm thin-film ^{6}LiF planar device operated under the same conditions as the perforated devices.

IV. Results

The ^{3}He calibrated thermal neutron flux was previously verified by measuring the neutron detection efficiency of a thin-film ^{6}LiF planar device and comparing against theory [4]. At a reverse bias of 3 volts, the neutron detection efficiencies for the devices with 200 μm deep perforations were found to be lower than previous results for devices with 100 μm deep perforations [4]. By increasing the detector bias to 20 volts, the neutron detection efficiency improved, yet system noise degradation mandated the LLD to be increased, hence effectively lowering the neutron detection efficiency for reverse biases above 30 volts. In addition, the ^{60}Co gamma-ray irradiation data indicates that gamma rays are easily discriminated from neutron counts, mainly due to the relatively small gamma-ray attenuation coefficient of Si and the thin device interaction region.

A. Neutron Counting Efficiency

All perforated devices were tested in the same neutron beam location and with the same NIM electronics as thin-film planar and perforated devices from previous experiments [4]. The spectra for the 200 μm deep perforated devices are shown in Figs. 2–4. The measured thermal neutron detection efficiencies for each perforated device are shown in Table I.

Surprisingly, the observed thermal neutron detection efficiency was lower for the 200 μm deep perforations than

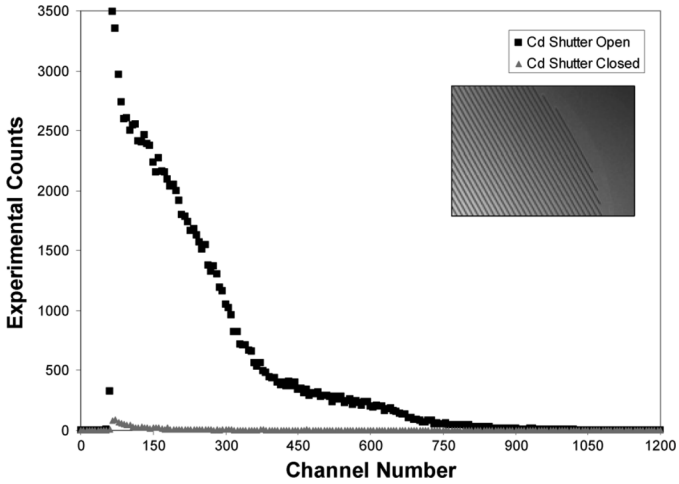

Fig. 3. Data for measured efficiency and spectral features for a straight trench perforated detector with 30 μm wide 200 μm deep trenches filled with ^{6}LiF.

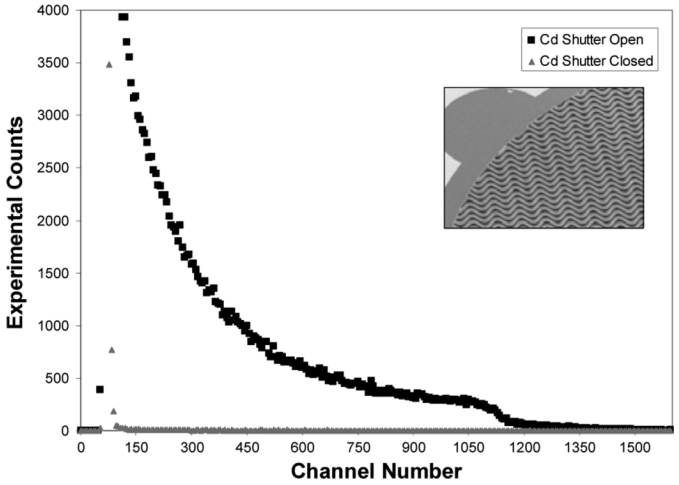

Fig. 4. Data for measured efficiency and spectral features for a sinusoidal trench perforated detector with 45 μm wave period 120 μm wave period 200 μm deep trenches filled with ^{6}LiF.

TABLE I
MEASURED NEUTRON DETECTION EFFICIENCIES

Perforation Type	Hole Depth	LLD	^{6}LiF Projected Area Density	Neutron Counting Efficiency
Circular Hole	200 μm	150	20 mg/cm^2	9.7 (± 0.4) %
Straight Trench	200 μm	150	26 mg/cm^2	12.6 (± 0.6) %
Sinusoidal Trench	200 μm	150	29 mg/cm^2	16.2 (± 0.9)%

observed for devices with 100 μm deep perforations [4], a result that first appears to be contrary to expectations [1]–[4]. It is believed that excessive contamination and/or mechanical damage to the base diode from etching the increased perforation depths has caused the depletion depth to be compromised. Hence, the actual depleted active depth of the detectors is less for the 200 μm deep perforated devices than the previous 100 μm deep perforated devices.

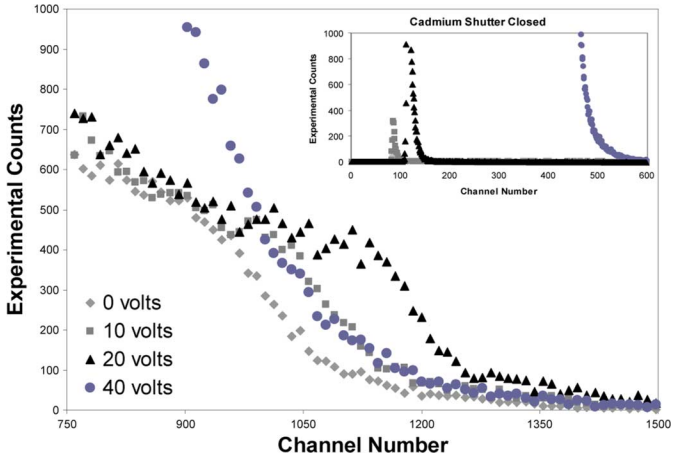

Fig. 5. Measured spectral features for a sinusoidal trench perforated detector at varying reverse bias voltages. Also shown is a plot of the cadmium covered spectrum, exemplifying the increase in system noise at 40 volts reverse bias.

The neutron detection efficiency as a function of increasing reverse bias was studied. If the Si device active region does not extend beyond the perforation depth at 3 volts, then the total count rate and neutron detection efficiency, will increase as the reverse bias is increased. Further, if the active region depth is less than the particle ranges at a reverse bias of 3 volts, then the energy distribution in the spectrum will also shift to higher channels as the reverse bias is increased.

Notice, from Fig. 5, that the neutron response spectrum is seen to shift towards higher energies as the reverse bias is increased. This confirms that the device is not fully depleted at 3 volts, and the reduction in efficiency is due to the reduction of the depletion depth as compared to previous 100 μm deep perforated devices [4]. Therefore, to increase the detection efficiency of the 200 μm deep perforated devices, the bias voltage must be increased. As a result of excessive electronic noise from the increased contamination and mechanical damage to the diode, the LLD must be increased, which offsets gains in efficiency expected from the increased perforation and depletion depths. For a reverse bias of 20 volts, and an LLD at channel 150, the measured thermal neutron detection efficiency increased to 19% for the sinusoid devices. However, a decrease in efficiency is observed (down to 12%) at a reverse bias of 40 volts, with the LLD set up to channel 600.

B. Perforated Neutron Detector ^{60}Co Irradiation Response

As a benchmark, a ^{60}Co irradiation response for a thin-film planar device was measured. The same procedure was used to measure the gamma-ray response of the circular hole, straight trench, and sinusoidal trench perforated devices. The gamma-ray response of each device is plotted with the neutron response for comparison, as shown in Figs. 6–9.

Gamma-ray discrimination is an important feature of the perforated detector design. Initial gamma-ray response of the perforated detectors was evaluated from the Cd prompt capture gamma-ray irradiation during the 'closed cadmium shutter' measurement, where the salient gamma-ray emissions are at 558.6 and 651.3 keV [12]; the spectra for the gamma-ray irradiations are shown in Figs. 2–4. To evaluate a higher energy

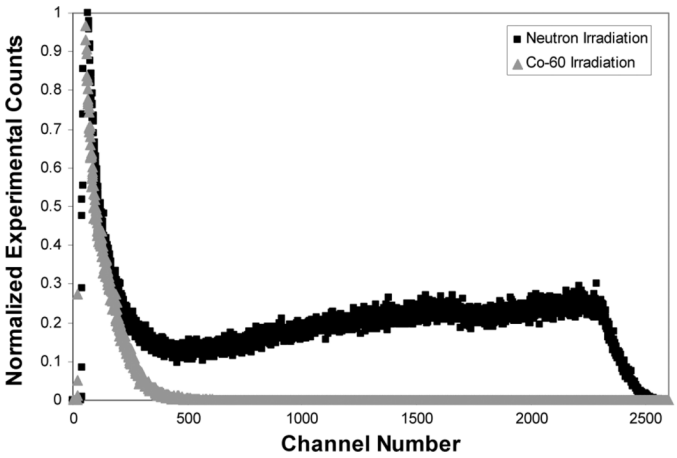

Fig. 6. Measured ^{60}Co gamma-ray irradiation and neutron irradiation spectral features for a planar detector with a 26 μm ^{6}LiF cap layer.

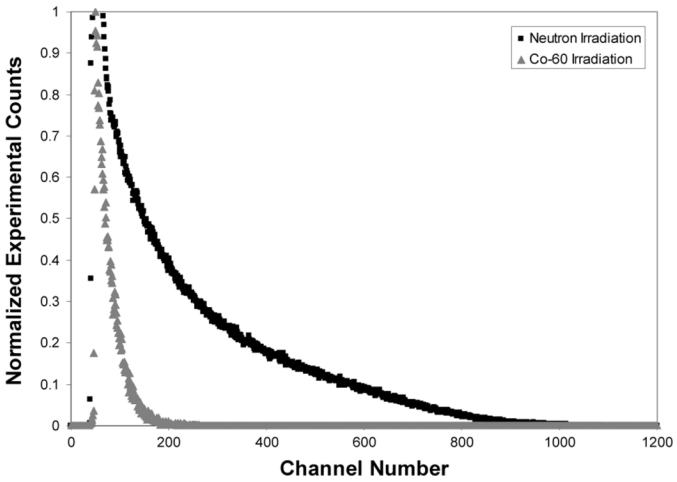

Fig. 7. Measured ^{60}Co gamma-ray irradiation and neutron irradiation spectral features for a circular hole perforated detector with 30 μm diameter 200 μm deep holes filled with ^{6}LiF.

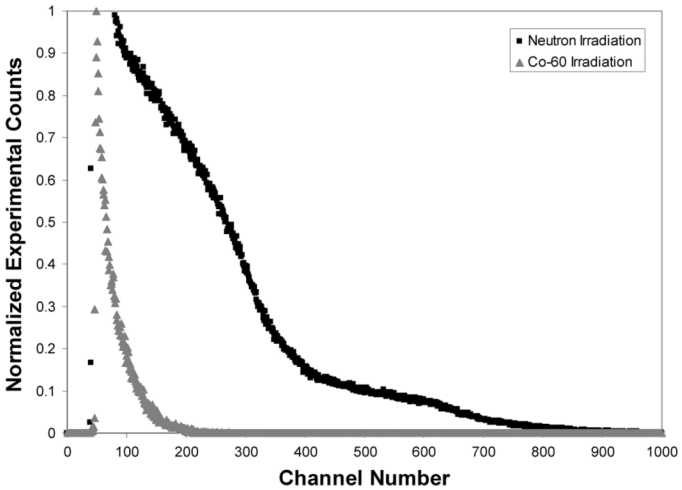

Fig. 8. Measured ^{60}Co gamma-ray irradiation and neutron irradiation spectral features for a straight trench perforated detector with 30 μm wide 200 μm deep trenches filled with ^{6}LiF.

gamma-ray response of the perforated neutron detectors, a ^{60}Co irradiation response was measured. The high-energy gamma

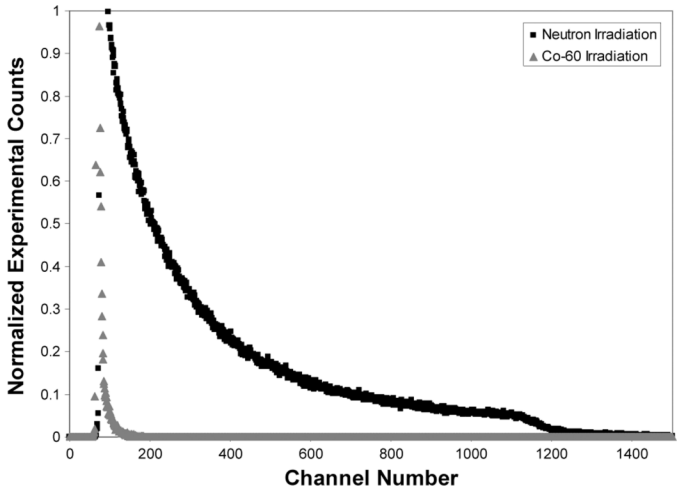

Fig. 9. Measured ^{60}Co gamma-ray irradiation and neutron irradiation spectral features for a sinusoidal trench perforated detector with 45 μm wave period 120 μm wave period 200 μm deep trenches filled with ^{6}LiF.

rays of ^{60}Co were easily discriminated from neutron counts, as the counts accumulated near the low energy section of the neutron reaction product spectrum. Specifically, more neutron counts can be integrated into the total observed with confidence, mainly because the LLD setting can be lowered, therefore increasing actual neutron counting efficiency. Also, the advantage of using ^{6}LiF as the neutron absorber material becomes clear, in which the higher energies from the ^{6}Li(n,T)^{4}He reaction are much higher than the reaction product energies from other commonly used materials such as ^{10}B and ^{157}Gd. Hence, the signal to noise and signal to gamma-ray response will be much smaller for devices using ^{10}B and ^{157}Gd absorber materials than devices using ^{6}LiF converters, therefore effectively reducing the neutron counting efficiency of ^{10}B and ^{157}Gd coated devices below that of ^{6}LiF coated devices [3]–[5].

V. Conclusion

In an attempt to increase the perforated neutron detector's detection efficiency, the perforation depths were increased from 100 μm to 200 μm. The increase in depth resulted in a decrease in neutron counting efficiency as compared to previous 100 μm perforated devices. It is speculated that the contamination and damage from the increased in perforation depth etching process caused a decrease in depletion width at 3 volts and therefore a reduction in detection efficiency. Upon increasing the reverse bias, which increases the depletion depth, the neutron detection efficiency noticeably increased from 16% at 3 volts reverse bias to 19% at 20 volts reverse bias. As the voltage was increased to 40 volts, increasing system noise made it necessary to increase the LLD setting, which resulted in an effective decrease in neutron counting efficiency. Regardless, 19% efficiency is over four times greater than can be achieved with a common planar device coated with ^{6}LiF [12]. Further work will be pursued to reduce damage during the etching process, thereby decreasing the noise of the perforated detectors, which appears to be the limiting factor of the device performance in neutron detection efficiency.

The perforated neutron detector demonstrates all of the advantages of solid-state electronic devices including: low voltage operation, compact, high neutron counting efficiency, fast timing response, and a wide field of view. Thus, the perforated detectors are ideal for dosimetry and monitoring applications [8]. An additional feature of the perforated neutron detectors is a high neutron to gamma-ray discrimination ratio. Finally, being semiconductor devices, the detectors can be mass-produced by typical VLSI techniques, hence greatly lowering unit cost.

ACKNOWLEDGMENT

This work was supported by DTRA, the National Science Foundation, and the US Department of Energy NEER. All detector design, fabrication, and characterization were performed at the Kansas State University SMART Laboratory.

REFERENCES

[1] J. K. Shultis and D. S. McGregor, "Efficiencies of coated and perforated semiconductor neutron detectors," *IEEE Trans. Nuclear Science*, vol. NS-53, pp. 1659–1665, 2006.

[2] W. J. McNeil, S. L. Bellinger, T. C. Unruh, E. L. Patterson, J. K. Shultis, and D. S. McGregor, "Perforated diode fabrication for neutron detection," in *IEEE NSS Conf. Record*, San Diego, CA, Oct. 29–Nov. 3 2006, pp. 3732–3735.

[3] J. Uher, C. Fröjdh, J. Jakůbek, C. Kenney, Z. Kohout, V. Linhart, S. Parker, S. Petersson, S. Pospíšil, and G. Thungström, "Characterization of 3D thermal neutron semiconductor detectors," *Nucl. Instrum. Meth. A.*, vol. 576, pp. 32–37, 2007.

[4] S. L. Bellinger, W. J. McNeil, T. C. Unruh, and D. S. McGregor, "Angular response of perforated silicon diode high efficiency neutron detectors," in *IEEE NSS Conf. Record*, Waikiki, Hawaii, Oct. 28–Nov. 3 2007, pp. 1904–1907.

[5] R. J. Nikoli, A. M. Conway, C. E. Reinhardt, R. T. Graff, T. F. Wang, N. Deo, and C. L. Cheung, "Fabrication of pillar-structured thermal neutron detectors," in *IEEE NSS Conf. Record*, Waikiki, Hawaii, Oct. 28–Nov. 3 2007, pp. 1577–1580.

[6] C. J. Solomon, J. K. Shultis, and D. S. McGregor, "Angular design considerations for perforated semiconductor detectors," in *IEEE NSS Conf. Record*, Waikiki, Hawaii, Oct. 28–Nov. 3 2007, pp. 1556–1559.

[7] D. S. McGregor, S. Bellinger, D. Bruno, W. L. Dunn, W. J. McNeil, E. Patterson, B. B. Rice, J. K. Shultis, and T. Unruh, "Perforated diode neutron detector modules fabricated from high-purity-silicon," *Radiation Physics and Chemistry*, 2007.

[8] Q. Jahan, E. Patterson, B. Rice, W. L. Dunn, and D. S. McGregor, "Neutron dosimeters employing high-efficiency perforated semiconductor detectors," *Nucl. Instrum. Meth. B.*, vol. 263, pp. 183–185, 2007.

[9] D. S. McGregor, S. L. Bellinger, D. Bruno, S. A. Cowley, W. L. Dunn, M. Elazegui, A. Kargar, W. J. McNeil, H. Oyenan, E. Patterson, J. K. Shultis, G. Singh, C. J. Solomon, and T. C. Unruh, "Wireless neutron and gamma-ray detector modules for dosimetry and remote monitoring," in *IEEE NSS Conf. Record*, Waikiki, Hawaii, Oct. 28–Nov. 3 2007, pp. 808–812.

[10] W. J. McNeil, S. L. Bellinger, B. J. Blalock, C. L. Britton, Jr., J. L. Britton, S. C. Brunch, S. A. Cowley, C. M. Henderson, T. J. Sobering, R. D. Taylor, and D. S. McGregor, "Preliminary tests of a high efficiency 1-D silicon pixel array for small angle neutron scattering," in *IEEE NSS Conf. Record*, Waikiki, Hawaii, Oct. 28–Nov. 3 2007, pp. 2340–2342.

[11] D. S. McGregor, R. T. Klann, H. K. Gersch, E. Ariesanti, J. D. Sanders, and B. VanDerElzen, "New surface morphology for low stress thin-film coated thermal neutron detectors," *IEEE Trans. Nucl. Sci.*, vol. 49, no. 4, pp. 1999–2004, Aug. 2002.

[12] D. S. McGregor, M. D. Hammig, H. K. Gersch, Y. H. Yang, and R. T. Klann, "Design considerations for thin film coated semiconductor thermal neutron detectors, part I: Basics regarding alpha particle emitting neutron reactive films," *Nucl. Instrum. Meth. A.*, vol. 500, pp. 272–308, 2003.

[13] D. S. McGregor and J. K. Shultis, "Spectral identification of thin-film coated and solid-form semiconductor neutron detector," *Nucl. Instrum. Meth. A.*, vol. 517, pp. 180–188, 2004.

[14] S. Pospisil, B. Sopko, E. Harrankova, Z. Janout, J. Konicek, I. Macha, and J. Pavlu, "Si diode as a small detector of slow neutrons," *Radiat. Protection Dosimetry*, vol. 46, pp. 115–118, 1993.

[15] C. Petrillo, F. Sacchetti, O. Toket, and N. J. Rhodes, "Solid state neutron detectors," *Nucl. Instrum. Meth. A.*, vol. 378, pp. 541–551, 1996.

[16] A. Mireshghi, G. Cho, J. S. Drewery, W. S. Hong, T. Jing, H. Lee, S. N. Kaplan, and V. Perez-Mendez, "High efficiency neutron sensitive amorphous silicon pixel detectors," *IEEE Trans. Nucl. Sci.*, vol. NS-41, no. 4, pp. 915–921, Aug. 1994.